Computing and Informatics, Vol. 33, 2014, 175–196

ILLUMINATION CORRECTION ON BIOMEDICAL IMAGES

Edoardo Ardizzone, Roberto Pirrone, Orazio Gambino

Department of Chemical, Management, Computer and Mechanical Engineering
University of Palermo, Viale delle Scienze, Building 6, Palermo, Italy
e-mail: {edoardo.ardizzone, roberto.pirrone, orazio.gambino}@unipa.it

Salvatore Vitabile

Department of Biopathology, Medical and Forensic Biotechnologies
University of Palermo, Via del Vespro 129, 90127 Palermo, Italy
e-mail: salvatore.vitabile@unipa.it

Abstract. RF-Inhomogeneity Correction (aka bias) artifact is an important research field in Magnetic Resonance Imaging (MRI). Bias corrupts MR images altering their illumination even though they are acquired with the most recent scanners. Homomorphic Unsharp Masking (HUM) is a filtering technique aimed at correcting illumination inhomogeneity, but it produces a halo around the edges as a side effect. In this paper a novel correction scheme based on HUM is proposed to correct the artifact mentioned above without introducing the halo. A wide experimentation has been performed on MR images. The method has been tuned and evaluated using the simulated Brainweb image database. In this framework, the approach has been compared successfully against the Guillemaud filter and the SPM2 method. Moreover, the method has been successfully applied on several real MR images of the brain (0.18 T, 1.5 T and 7 T). The description of the overall technique is reported along with the experimental results that show its effectiveness in different anatomical regions and its ability to compensate both underexposed and overexposed areas. Our approach is also effective on non-radiological images, like retinal ones.

Keywords: RF-inhomogeneity, MRI, magnetic resonance, homomorphic unsharp masking, bias artifact

1 INTRODUCTION

Recent advances in medical image processing are oriented to mobile applications [1] and human-computer interaction [2] during the diagnostic process. RF-Inhomogeneity correction represents an interesting open issue in Magnetic Resonance Imaging (MRI). RF-Inhomogeneity is produced by fluctuations of the radiofrequency (B1) magnetic field. The corruption, also called bias artifact, alters the brightness with an unknown law, depending on hardware configuration, scanning sequence, tissue type, and other complex parameters. Bias is different from the classical noise, since it corrupts low harmonics. Several methods have been proposed to correct RF-Inhomogeneity. Existing methods can be divided into

1. pattern recognition methods,
2. polynomial fitting techniques,
3. methods requiring special experimentation, and
4. homomorphic unsharp masking methods (HUM).

HUM is a filtering scheme that is aimed at correcting bias artifact. Unfortunately, it produces collateral haloes around the image edge. In this paper, a new approach, called Halo Compensated Homomorphic Unsharp Masking (HC-HUM), is presented. The proposed approach is a refinement of the classic homomorphic filter, because it removes over-illumination artifacts along boundary regions. The idea behind the proposed elaboration pipeline consists in performing a gray level correction on the highest portion of the image dynamics thanks to a non-linear gray level mapping and a dynamics recovery process. Starting from the results obtained by some of the authors in a previous work [30] the contrast stretching block in the Guillemaud's scheme [22] has been replaced by a couple of blocks devoted to non-linear gray levels mapping and dynamics recovery. Such a solution restores the image from the halo produced by internal edges, while the previous work did not remove internal haloes. A wide quantitative experimentation of the proposed method has been performed on the Brainweb simulated MR image database. Next, the method has been applied successfully to both ultra high-field (7 T) MR images and non-MR images like retinal ones to assess its effectiveness in different domains.The paper is organized as follows. Section 2 reports the main related works addressing RF-Inhomogeneity and halo artifact. Section 3 describes the corruption model where the homomorphic principle is introduced, while the proposed correction model is presented in Section 4. A wide experimentation on biomedical images with objective measures confirming the effectiveness of our approach is presented in Section 5. Finally, Section 6 reports conclusions.

2 RELATED WORKS

As stated in the previous section, several techniques have been proposed in the literature to face RF-inhomogeneity correction. Classical statistical pattern recognition

approaches are useless since typical MR data are corrupted, so that the mean value of a tissue varies depending on its position. As a result, such methods need to add new terms to their original objective function in order to address the data fluctuations issue. The objective function of the fuzzy c-means algorithm [3] also considers the mean value of the pixel neighbors that is weighted by a new parameter and is used to replace the corrupted image with the value obtained from the degradation model [4]. A more complex definition of the objective function is introduced in [5]. The new terms introduce fluctuations to the first and second order finite differences at each pixel and they are weighted through two parameters. In general, modified methods require more computational resources than the original ones, since the centroids and memberships vectors have some new terms. Values for new parameters are unknown and they can be obtained through empirical considerations aimed at restoring a particular dataset. A new method described in [6] differs from the method [5] because the original fuzzy c-means algorithm is used to find initial values for the centroids and memberships vectors. The Expectation Maximization has been modified to compensate the RF-Inhomogeneity. The initial assumption is that the probability function of the data can be represented as a Gaussian mixture, so that each portion of the total population belongs to a Gaussian with a suitable mean value and standard deviation. In [7] a modified version is proposed modeling the RF-Inhomogeneity as a linear combination of smoothing functions. A new processing step has been added that requires computing the coefficients of the linear combination. The work reported in [8] assumes that the tissues and bias classes are statistically independent. The bias is modeled through a Gaussian function with zero mean value and the previous assumptions are used to modify the EM steps. The method has been further modified in [9]. In this work the authors consider a portion of population with a uniform distribution function. The segmentation method reported in [10] uses a modified version of the Hidden Markov Models to segment an image corrupted by illumination variation. This approach is called Hidden Markov Random Field and consists of a stochastic process considering two random families, while the RF-Inhomogeneity is compensated using a method similar to the method proposed in [9]. In other works, RF-Inhomogeneity is approximated by an interpolating surface whose parameters are determined using statistical methods. In the PABIC (PArametric BIas Field Correction) method [11, 27] the corruption is modeled using the Legendre polynomials. The image is thought as composed by large uniform patches representing each tissue, and it requires a pre-segmentation phase to determine the mean value, the standard deviation, and a binary mask for each patch. Legendre polynomials are fitted following an iterative optimization algorithm called (1+1)ES (Evolution Strategy). In [12] image corruption is modeled using B-Spline surfaces whose parameters are determined using an iterative algorithm. The method stops when the ratio between standard deviation and the mean value computed on the estimated corruption is less than a fixed threshold. This method was called N3. The method reported in [13] is an iterative algorithm composed by merging N3 and a gray levels histogram correction model to overcome the performance of N3 when the artifact is particularly strong. A different strategy to

estimate the bias artifact starts from the insertion of a special probe (aka phantom) into the device to acquire an image representing only the bias distribution. Once the volume representing the artifact has been acquired, it is modeled as a quadratic 3D polynomial using the Singular Value Decomposition [14]. The polynomial can be used to correct a corrupted volume using a homomorphic-like process. A thin plate surface model is used in [15] to obtain the correction surface. The method does not correct volumetric data. The thin plate surface is fitted on some control points, which are selected manually on the phantom image. Selected points are then used to train a neural network also using pre-segmented images of the brain. The technique presented in [34] corrects non-homogenous illumination in retinal images, and makes use of B-splines to approximate the shading model. The works cited above are based on the Homomorphic Unsharp Masking (HUM) described in [16]. In this method, a log function is applied to the corrupted image and its blurred version is subtracted from the previous result. Finally, an exponential function is applied to the resulting image. In [17] a comparison between mean and median filters is made to estimate the unsharp mask and it is used to correct brain MR volumes in [18]. In [28, 29, 30] homomorphic filtering is refined with foreground information extraction and automatic cut-off frequency selection through the analysis of the bias entropy curve. In [32] a method to correct intensity inhomogeneity in MR images subject to strong shading artifact is presented. Strong shading is due to the presence of phased array RF reception coils such as in vascular imaging of the neck for atherosclerosis diagnosis. The bias field is modeled with a cubic spline and the entropy of the corrected image is minimized locally. The authors called this new method Local Entropy Minimization with cubic Spline model (LEMS). In [33], LEMS is compared to a modified fuzzy c-means segmentation based method (mAFCM) and a linear filtering method (LINF). In the physical phantom used by the authors, LEMS reduced the overall variation in the image to 1.9 %, and to 2.5 % across the vessel wall region. In [19] some of the methods described above have been evaluated and compared against a brain MRI dataset. The main problem in HUM is the introduction of a new artifact along the boundary between two regions with different intensity. It is known as overshoot or halo artifact. In [18], this problem is mentioned explicitly but it is solved by surrounding the encephalic region with a gray uniform background before applying the homomorphic filter. Obviously, this operation requires an accurate pre-segmentation of the brain area in each slice. A more detailed description of this process is reported in [20]. In [31] a low-frequency model is adopted to estimate the bias by means of low-pass filtering. Low-pass filtering methods denote high speed and low computation complexity but limited efficiency due to the edge effects related to high image contrasts. The authors use two preprocessing filters (Wiener and Gaussian filters) to overcome some of the current limitations of lowpass frequency models for bias correction in MR images. Tests (qualitative validation) concern high-field (9.4 T) surface coil brain images of the rat since the bias in such data makes their visual inspection and computer vision technique analysis very difficult if not impossible. Other HUM based methods do not mention this problem.

3 THE CORRUPTION MODEL

Two main artifacts corrupt the MR image: RF-Inhomogeneity and noise. From the point of view of the frequency domain, the former alters the low frequency harmonics, while the latter corrupts the high frequencies. In the spatial domain, the RF-Inhomogeneity is a multiplicative corruption while the noise is an additive one [11, 12, 23]. On the basis of the features depicted above, we can write the following corruption model:

$$I_c = I \cdot B + N. \tag{1}$$

The corrupted image I_c is obtained by the sum of the noise (N) and the artifacts free image (I) that is multiplied by the RF-Inhomogeneity corruption (B). The noise can be suppressed using current noise removal filters, such as anisotropic diffusion filter [21]; moreover, we shall follow a frequency domain approach to restore I_c, so just the terms I and B will be considered, because only the low frequency harmonics will be filtered. Computing the natural logarithm of both members in Equation (1), an additive corruption is obtained:

$$\ln(I_c) = \ln(I) + \ln(B). \tag{2}$$

Now the corruption $\ln(B)$ can be estimated applying a low-pass (LP) filter on $\ln(I_c)$:

$$\ln(B) = LP(\ln(I_c)). \tag{3}$$

Substituting the (3) into (2) we obtain:

$$\ln(I_c) = \ln(\hat{I}) + LP(\ln(I_c)). \tag{4}$$

So we obtain the following estimation of the uncorrupted logarithmic image:

$$\ln(\hat{I}) = \ln(I_c) - LP(\ln(I_c)). \tag{5}$$

In order to obtain the estimated restored image, the $\exp(\cdot)$ function must be applied to both the members of (5) obtaining:

$$\hat{I} = \exp(\ln(I_c) - LP(\ln(I_c))). \tag{6}$$

4 HALO COMPENSATED HOMOMORPHIC UNSHARP MASKING

Equation (6) is the basis of the homomorphic filter (hf), whose block diagram is presented in Figure 1 a). Often a biomedical image is composed by two macro-regions: a very dark background and a light foreground (see Figure 2 a)–b)). The image resulting from the application of the homomorphic filter exhibits a halo artifact around the boundaries between the two macro-regions (see Figure 2 c)). This issue has been faced in [30] using the Guillemaud scheme [22], summarized in the Figure 1 b) as a block diagram.

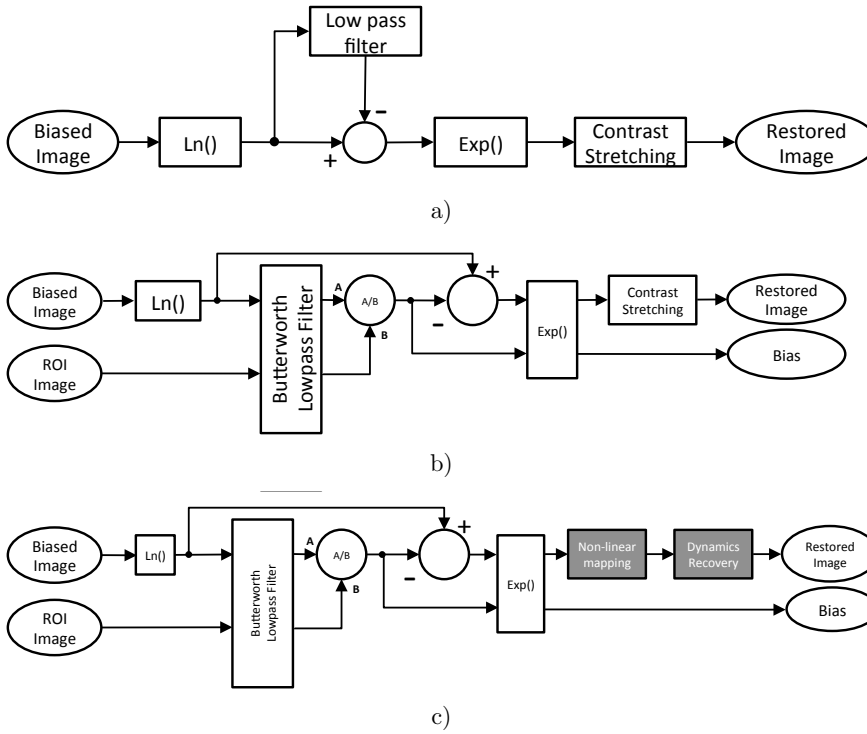

Figure 1. Classic homomorphic unsharp masking scheme a); Guillemaud scheme b); HCHUM c).

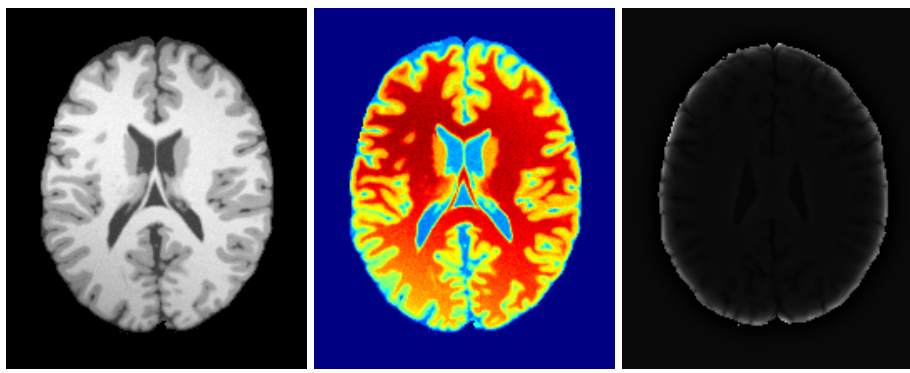

a) b) c)

Figure 2. A 70 % RF-Inhomogeneity corrupted image of the brain from Brainweb database a), its false colors version b); the halo arises when a common homomorphic filter is applied to the image c).

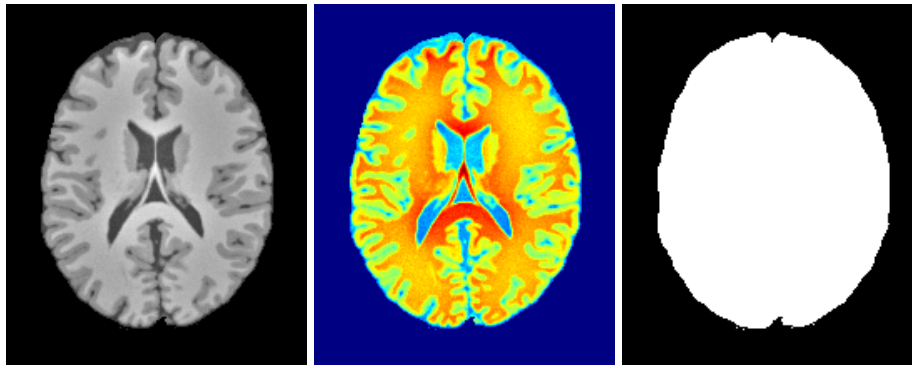

a) b) c)

Figure 3. Guillemaud based restoration of the image in Figure 2 a) a); the same image in false colors: red-shift points out the halo artifact b); the ROI image used for the Guillemaud scheme c)

It makes use of a binary image representing the Region of Interest (ROI), shown in (see Figure 3 c)), to compensate the halo artifact between foreground and background when a common homomorphic filter is applied to an image with a dark background. The resulting image is shown in Figure 3 a)–b). The Halo Compensated Homomorphic Unsharp Masking (HC-HUM) restoration scheme proposed in this work (see Figure 1 c)) tries to compensate the internal haloes without a segmentation task by means of a new halo compensation task, which is placed after the proper Guillemaud scheme [22]. Indeed, the Guillemaud filter is not able to suppress the halo located on the boundaries between a dark tissue and a light one. In previous works proposed by some of the authors [30] internal haloes did not appear because the Cerebrospinal Fluid (CSF), which is the darkest tissue of a T1-weighted MR brain image, was removed by segmentation. As a consequence, a more accurate ROI definition was required in such a way that the ROI had gaps and/or holes in correspondence to the CSF. In the present work the authors suppose that once the halo between foreground and background is removed, the most intense halo is localized on the boundary between the ventricular system, where CSF flows inside, and the white matter (WM), which is the lightest tissue of the brain. Under this hypothesis, the halo arising in the WM corrupts the highest part of the image dynamics, so an appropriate gray mapping is sufficient to restore the WM intensity. The non-linear intensity mapping law is expressed by the following equation:

$$y(x) = x - k \cdot \ln\left(\sqrt{1 + \left(\frac{x}{x_t}\right)^m}\right). \tag{7}$$

This mapping law is designed to follow the shape of the $y = x$ straight line for low intensity values, while the output intensity is reduced in the upper part of the

gray levels range. Such a non linear mapping is applied to the image E obtained from the exponential function in the HC-HUM scheme (Figure 1 c)). The curve starts about at $0.1 \cdot x_t$, because it is quite similar to a pole formula of the Bode magnitude plot in the Systems Theory. The m exponent characterizes the global shape of the curve, while the k coefficient is a gain factor acting on its curvature. The effect of each parameter on the curve is showed in Figure 4.

Let G be the image obtained as the output of the intensity mapping. The intensity of G is normalized to the original image gray level dynamics, so that the restored image R is obtained as follows:

$$R = \frac{G - \min(G)}{\max(G) - \min(G)} \cdot \frac{\max(G)}{\max(E)} \cdot \max(I). \tag{8}$$

Five parameters have to be set in HC-HUM. The Butterworth lowpass filter needs the cut-off frequency f_t and the order to be tuned, while the intensity mapping curve requires tuning k, m, x_t. The cut-off frequency can be selected by the local entropy curve defined in [30] and the filter order can be set to 1. The gain factor k is usually a value in the interval $(0, 1]$ because the curve cannot attenuate the intensities dramatically. For the same reasons, acceptable values of the exponent m are comprised in the interval [2,8] because it could cause an abrupt rotation around a point as it can be seen in Figure 4. The value of x_t must be close to the upper limit of the dynamics, where the halo intensity is located. The restored image in Figure 5 is obtained with the following parameters: $f_t = 0.015$, $k = 1$, $x_t = 1.38$, $m = 4$. The method can be extended easily to 3D version, allowing to process entire volumes, if required, instead of a single image.

5 EXPERIMENTAL RESULTS

Several experiments have been carried out to assess the effectiveness of the proposed method. HC-HUM has been compared with other state-of-the-art approaches on the Brainweb simulated database, and quantitative performance measures have been extracted in this case because such a database also provides the segmented tissues for each slice. As a consequence, we were able to make an explicit estimation of the amount of correction.

HC-HUM has been also tested on several real datasets coming from MR devices with varying coil arrangement and different magnetic field strength. In this case we did not have segmented slices and a global correction measure is useless to assess the effectiveness of the method as RF-Inhomogeneity produces unpredictable spatial fluctuations in image intensity. Moreover, haloes are located in each slice along the boundaries between tissues so a global measure does not take into account the compensation effect discussed in this work. Direct inspection by a team of radiologists has been used in these cases to achieve a qualitative evaluation.

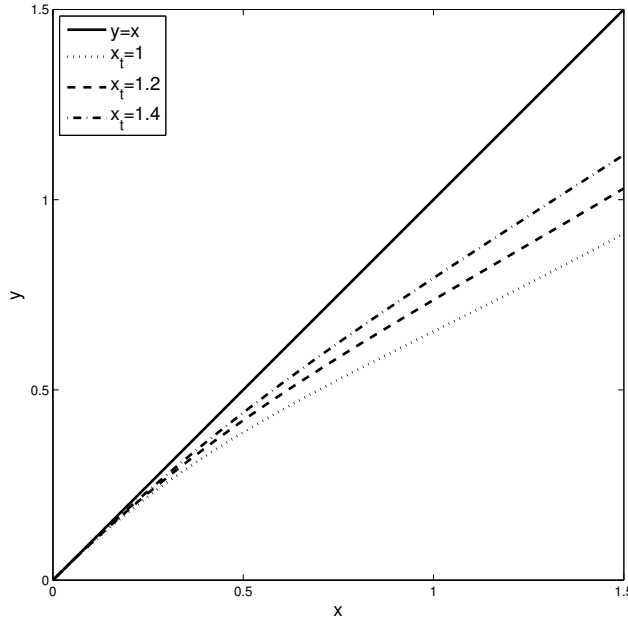

a)

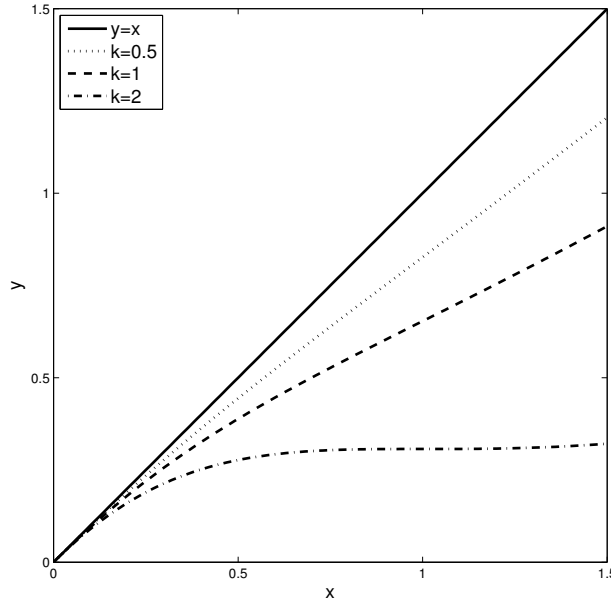

b)

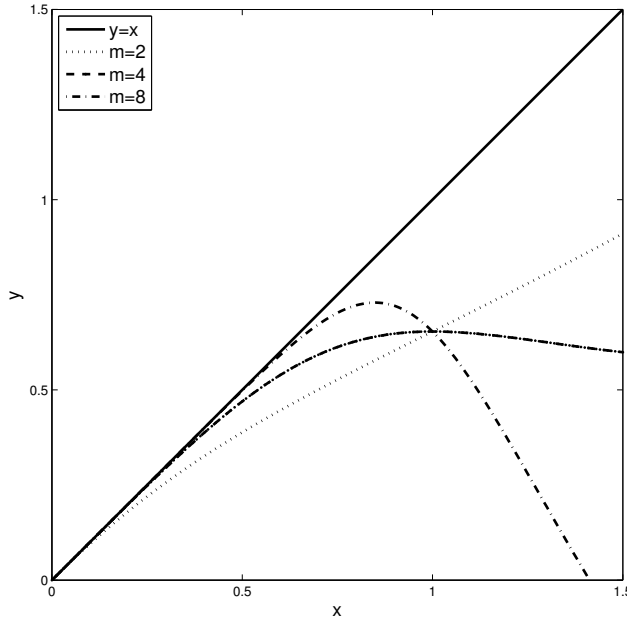

c)

Figure 4. The effect of each parameter on the curve in Equation (7): a) x_t is varying, $k = 1$, $m = 2$; b) k is varying, $x_t = 1$, $m = 2$; c) m is varying, $k = 1$, $x_t = 1$

Finally, we tested the method on a retinal images dataset as well to gain hints about its generality as regards the image source, that is not only MRI. The following subsections deal with each experiment separately.

5.1 Brainweb Simulated Database

Brainweb [24, 25] is a simulated brain database freely available online. It provides RF-Inhomogeneity corrupted image whose amount of corruption can be set by the user. It also provides a correct segmentation of the macro tissues: white matter, gray matter, and cerebrospinal fluid. We used this database to validate the method. Three T1-weighted volumes with 20 %, 40 %, and 70 % of RF-Inhomogeneity corruption and 1 % of noise have been downloaded. The scanning parameters have been set to the default values: spoiled FLASH sequence, repetition time: 18 ms, echo time: 10 ms, flip angle: 30°, spatial resolution: 217×181 pixels, slice thickness: 1 mm.

The amount of removed RF-Inhomogeneity is measured by the coefficient of variation (cv). It is computed for each tissue and it consists in the ratio between its standard deviation σ and mean intensity μ:

$$cv = \frac{\sigma}{\mu}.$$

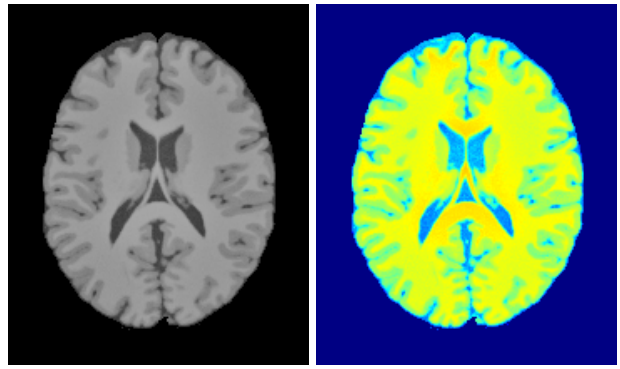

a) b)

Figure 5. The restored image using HC-HUM a) and its false color version b). The absence of the red-shift in the colored image implies the absence of the halo.

The performance of the 3D version of the HC-HUM has been compared to both the Guillemaud filtering scheme and the SPM2 algorithm. The *cv* values computed on the whole volumes are reported in Table 1. Figure 6 plots the *cv* computed for each 2D slice in the original (corrupted) case, after applying the Guillemaud filter, and after processing the slice with HC-HUM. The *cv* values of the proposed method are lower than the others.

5.2 0.18 T MRI Dataset

In this study we used 5 subjects acquisitions on an ESAOTE ARTOSCAN C, 0.18 Tesla. MR imaging was performed with the following key settings: spin echo sequence, repetition time: 980 ms, echo time: 26 ms, slice thickness: 4 mm, flip angle: 90°. The parameters used to restore the image: $f_t = 0.01$, $k = 1.2$, $x_t = 2.4$, $m = 8$. A visual example is shown in Figure 7.

5.3 1.5 T MRI Dataset

In this study we used 3 volunteer acquisitions on a Philips ECLIPSE 1.5 T. The pelvis and spinal cord dataset consists of images acquired with the following parameters: spoiled gradient echo sequence (steady state), repetition time: 10 ms, echo time: 3 ms, slice thickness: 10 mm, flip angle = 20 degrees. The parameters used to restore the images: $f_t = 0.03$, $k1 = 0.5$, $x_t = 1.5$, $m = 4$. A visual example is shown in Figure 8.

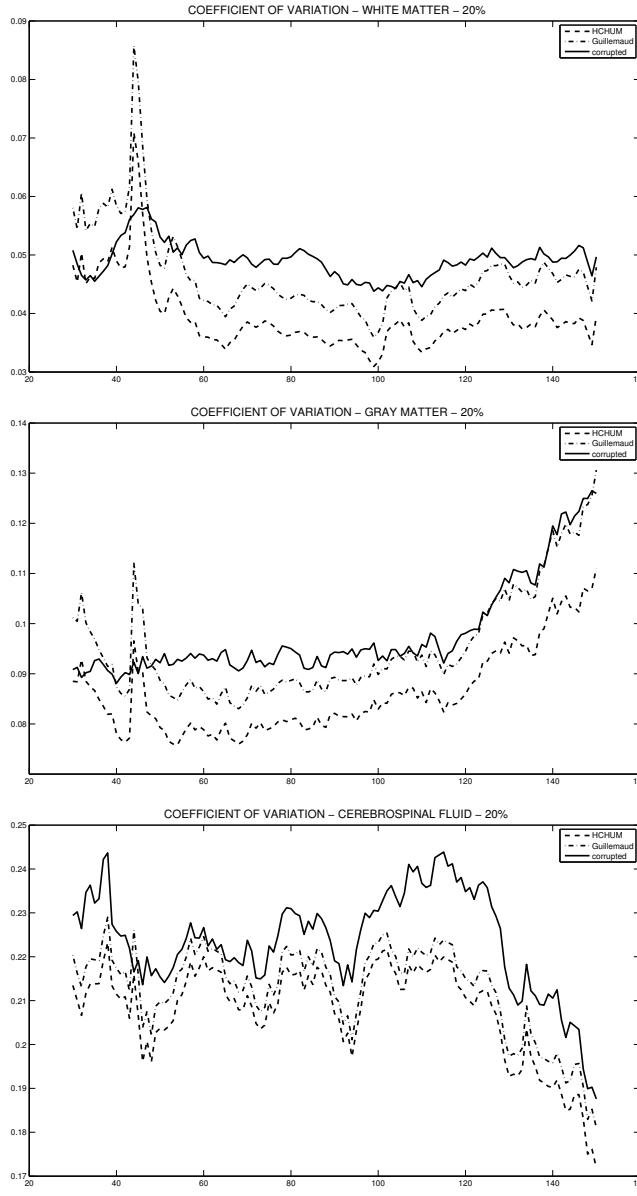
COEFFICIENT OF VARIATION – WHITE MATTER – 20%
HCHUM
Guillemaud
corrupted
COEFFICIENT OF VARIATION – GRAY MATTER – 20%
HCHUM
Guillemaud
corrupted
COEFFICIENT OF VARIATION – CEREBROSPINAL FLUID – 20%
HCHUM
Guillemaud
corrupted

a)

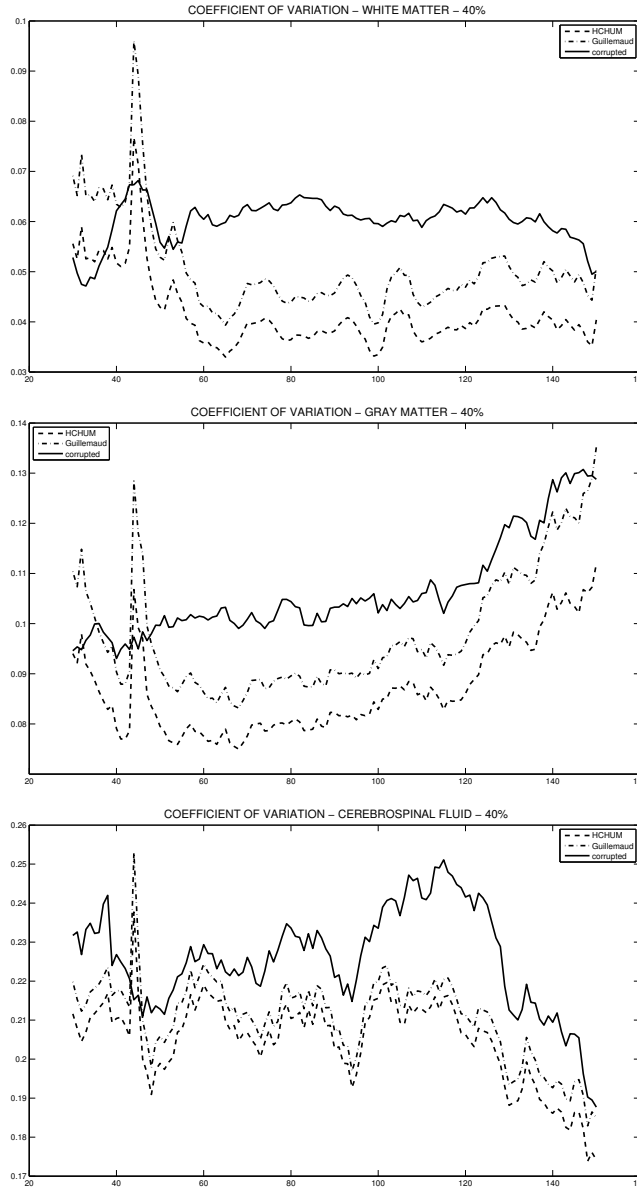
COEFFICIENT OF VARIATION – WHITE MATTER – 40%
HCHUM
Guillemaud
corrupted
COEFFICIENT OF VARIATION – GRAY MATTER – 40%
HCHUM
Guillemaud
corrupted
COEFFICIENT OF VARIATION – CEREBROSPINAL FLUID – 40%
HCHUM
Guillemaud
corrupted

b)

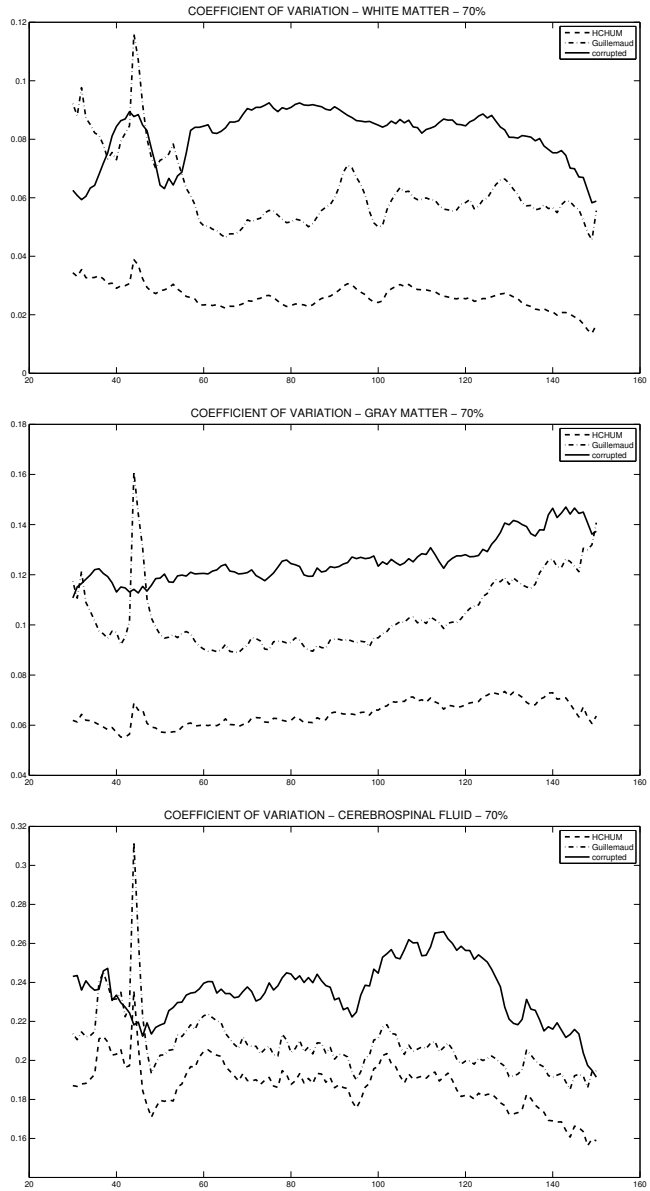

c)

Figure 6. The *cv* plotted for each Brainweb T1-weighted dataset corrupted by RF-Inhomogeneity a) 20 %, b) 40 %, c) 70 %. The 2D version of HC-HUM has been applied with the following parameters: (20 %) $f_t = 0.006$, $k = 0.35$, $x_t = 1.45$, $m = 4$; (40 %) $f_t = 0.008$, $k = 0.4$, $x_t = 1.45$, $m = 4$; (70 %) $f_t = 0.015$, $k = 1$, $x_t = 1.38$, $m = 4$.

Brainweb T1-weighted RF-Inhomogeneity (20 %)

	White Matter	**Gray Matter**	**CSF**
Guillemaud	0.0477	0.0933	0.2094
SPM2	0.0428	0.0915	0.2278
HC-HUM	0.0225	0.0784	0.2083

Brainweb T1-weighted RF-Inhomogeneity (40 %)

	White Matter	**Gray Matter**	**CSF**
Guillemaud	0.0472	0.0932	0.2089
SPM2	0.043	0.0917	0.2291
HC-HUM	0.0223	0.0785	0.2078

Brainweb T1-weighted RF-Inhomogeneity (70 %)

	White Matter	**Gray Matter**	**CSF**
Guillemaud	0.0505	0.0965	0.2121
SPM2	0.0454	0.0945	0.2352
HC-HUM	0.024	0.0813	0.211

Table 1. Values of the *cv* measure obtained for the Guillemaud filter, SPM2, and HC-HUM applied to an entire Brainweb volume with varying amount of RF-Inhomogeneity

5.4 7 T MRI Dataset

7 T ultra-high field MR images are strongly affected by radio-frequency (B1) magnetic field inhomogeneity. As a result, images are very noisy, even if they appear to be an outstanding clinical application. In this initial feasibility study we used a healthy volunteer acquisition on a Philips 7 T Achieva system to assess effec-

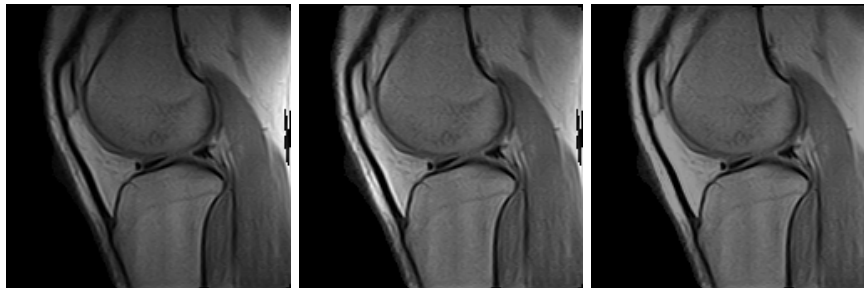

a) b) c)

Figure 7. A restoration example from the 0.18 T dataset: a) original image of a knee; b) image restoration using Guillemaud filtering; c) image restoration performed by HC-HUM

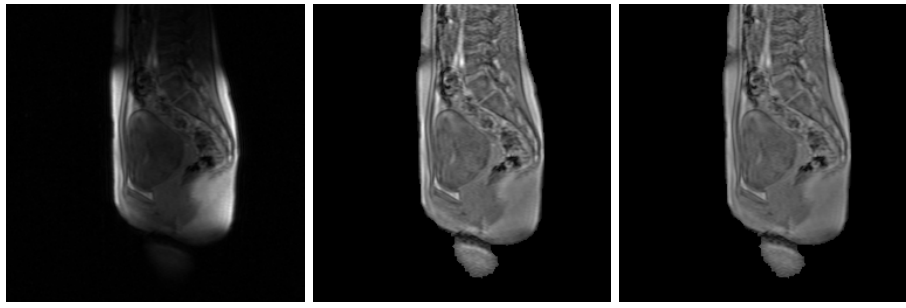

a) b) c)

Figure 8. A restoration example from the 1.5 T dataset: a) original image of a knee; b) image restoration using Guillemaud filtering; c) image restoration performed by HC-HUM

tiveness of the proposed filter. 7 T MR imaging was performed with the following key settings: 2D multi-slice; 60 slices; slice thickness = 1.5 mm; repetition time $[TR, ms] = 7.74$; echo time $[TE, ms] = 3.50$. The parameters used to restore the images: $f_t = 0.02$, $k1 = 0.3$, $x_t = 1.15$, $m = 5$. In Figure 9 a sample of a 7 T T1-weighted MR image of the brain is depicted along with its Guillemaud and HC-HUM restorations.

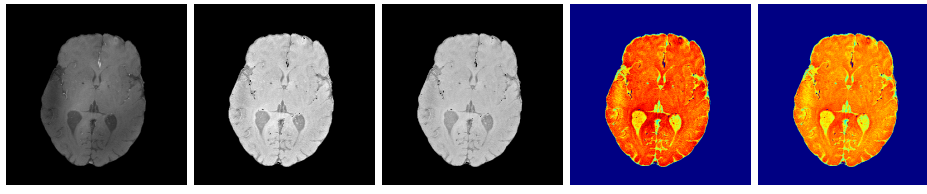

a) b) c) d) e)

Figure 9. A restoration example from the 7 T T1-weighted brain MR dataset: a) the original slice; b) the resulting image obtained applying the Guillemaud filter; c) restored image obtained applying HC-HUM; d) Figure 9 b) in false color; e) Figure 9 c) in false color. The red-shift (i.e. the halo color gamut) results to be more attenuated when using HC-HUM than in the Guillemaud case.

5.5 Retina Dataset

The DRIVE database has been established to enable studies on segmentation of blood vessels in retinal images. The images were acquired using a Canon CR5 non-mydriatic 3CCD camera with a 45 degree field of view (FOV). Each image was captured using 8 bits per color plane at 768 by 584 pixels. The FOV of each image is circular with a diameter of approximately 540 pixels. The parameter used to

restore the images are $f_t = 0.02$, $k = 0.55$, $x_t = 1.28$, $m = 8$. A visual example is shown in Figure 10.

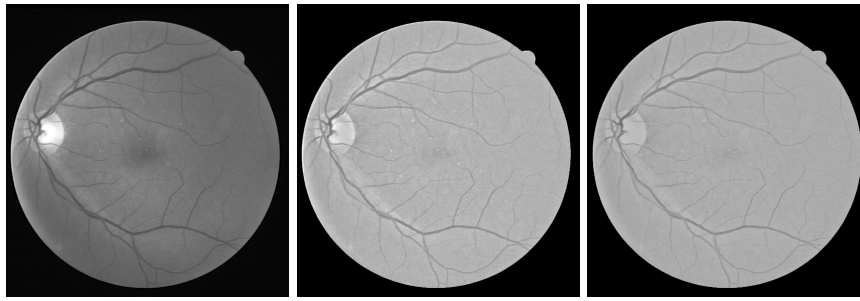

a) b) c)

Figure 10. A restoration example from the DRIVE retinal dataset: a) original image of a retina; b) the restored image using Guillemaud filtering; c) the restored image obtained by applying HC-HUM

6 DISCUSSIONS AND CONCLUSION

The HC-HUM filtering scheme presented in this paper is an image processing method which allows for compensating haloes in bias removal tasks. It can be used as an image enhancement CAD to help physicians findings. The method has been validated using the Brainweb image database, which is the international standard de facto for research in the field of MRI. The method has been applied successfully on several MR datasets with different magnetic field intensity (0.18 T, 1.5 T, and 7 T) as well as on retina images. HC-HUM requires very few parameters to be set. Some indications about their values and behavior are outlined in the paper. The method does not require any a priori information about processed images, tissues, and organs under investigation. Moreover, no a priori model of either the bias or the halo is required so that our method can be referred as a general purpose one. HC-HUM can work on a single image but it can be easily extended to volumetric data processing. This important feature has allowed for comparing the method against other techniques in the literature such as SPM2 [26], which operates only on volumes. Unlike other approaches, HC-HUM does not require complex iterative modules such as image registration, image segmentation, and artifact model estimation, so it does not require any specialized high computational intensive infrastructure. Moreover, HC-HUM does not require any normalization in the Talairach-Tourneaux reference system as well as any information about the spatial displacement, the orientation, and the geometry of the brain image under investigation. As stated before, the method has been first tested using the Brainweb image database. The achieved results show that the coefficient of variation resulting from HC-HUM application is the lowest among all the other methods. This implies that the brightness variation

inside a tissue (gray matter, white matter, and CSF) is low, so that bias and halo artifact are significantly reduced. As shown in the presented results, HC-HUM is more effective on the white matter, since it has the highest intensity level and the gray level mapping is designed to compensate the highest intensity levels in the dynamics. The same performance level is maintained when the method is applied on brain volumes.

Results show that HC-HUM reduces the corruption measured by the *cv* value on the WM by about 53 % when compared to the Guillemaud filter and by about 48 % when compared to the SPM2, while the reduction is about 16 % for the gray matter, and there is no reduction for the CSF. This is due to the method sensibility to the brightness of each region.

HC-HUM has been tuned on the Brainweb dataset, and tested against the real datasets described in the previous section. Applying HC-HUM to MR images results in a more uniform illumination distribution compensating both underexposed and overexposed areas that are due to the magnetic field inhomogeneity caused by the surface coils. Finally, retinal images exhibit brightness attenuation on the optical disk without any halo around the vessels. At the same time, the fovea results more illuminated. The features mentioned above result in a more effective application of the standard retina image segmentation and analysis algorithms.

Acknowledgments

The authors would like to thank Prof. M. Midiri and his research staff at the Dipartimento di Biopatologia e Biotecnologie Mediche e Forensi, University of Palermo, Italy for the 0.18 T knee images, Dr. E. Basilico, Dr. F. Longo, Dr. M. P. Pappalardo, and all the staff of Palermo's Ospedale Civico, Palermo, Italy for the 1.5 MRI images, Prof. Michael V. Knopp and his research staff at the Department of Radiology, The Ohio State University, Columbus, Ohio, USA for the 7 T MRI images.

REFERENCES

[1] Sorce, S.—Augello, A.—Santangelo, A.—Gentile, A.—Genco, A.—Gaglio, S.—Pilato, G.: Interacting with Augmented Environments. IEEE Pervasive Computing, Vol. 9, 2010, No. 2, pp. 57–58.

[2] Cannella, V.—Gambino, O.—Pirrone, R.—Vitabile, S.: GUI Usability in Medical Imaging. IEEE International Conference on Complex, Intelligent and Software Intensive Systems (CISIS) 2009, pp. 778–782, ISBN: 978-1-4244-3569-2, DOI:10.1109/CISIS.2009.87.

[3] Bezdek, J. C.: Pattern Recognition with Fuzzy Objective Function Algorithms. Plenum, NY 1981.

[4] Ahmed, M. A.—Yamany, S. M.—Mohamed, N.: A Modified Fuzzy CMeans Algorithm for Bias Field Estimation and Segmentation of MRI Data. IEEE Transactions on Medical Imaging. Vol. 21, 2002, pp. 193–199.

[5] Pham, D. L.—Prince, J. L.: Adaptive Fuzzy Segmentation of Magnetic Resonance Images. IEEE Transactions on Medical Imaging. Vol. 18, 1999, No. 9, pp. 737–752.

[6] Jiang, L.—Yang, W.: A Modified Fuzzy C-Means Algorithm for Segmentation of Magnetic Resonance Images. In Proc. 7th Digital Image Computing: Techniques and Applications,2003, Sun, C., Talbot, H., Ourselin, S. and Adriaansen, T. (Eds.), pp. 225–231.

[7] van Leemput, K.—Maes, F.—Vandermeulen, D.—Suetens, P.: Automated Model-Based Bias Field Correction of MR Images of the Brain. IEEE Transactions on Medical Imaging, Vol. 18, 1999, pp. 885–896.

[8] Wells, W. M.—Grimson, W. E. L.—Kikins, R.—Jolez, F. A.: Adaptive Segmentation of MRI Data. IEEE Transactions on Medical Imaging. Vol. 15, 1996, pp. 429–442.

[9] Guillemaud, R.—Brady, M.: Estimating the Bias Field of MR Images. IEEE Transactions on Medical Imaging, Vol. 16, 1997, pp. 238–251.

[10] Zhang, Y.—Brady, M.—Smith, S.: Segmentation of Brain MR Images Through a Hidden Markov Random Field Model and the Expectation Maximization Algorithm. IEEE Transactions on Medical Imaging, Vol. 20, 2001, No. 1, pp. 45–57.

[11] Styner, M.—Brechbuhler, C.—Szekely, G.—Gerig, G.: Parametric Estimate of Intensity Inhomogeneities Applied to MRI Medical Imaging. IEEE Transactions on Medical Imaging, Vol. 22, 2000, pp. 153–165.

[12] Sled, J. G.—Zijdenbos, A. P.—Evans, A. C.: A Nonparametric Method for Automatic Correction of Intensity Nonuniformity in MRI Data. IEEE Transaction Medical Imaging, Vol. 17, 1998, pp. 87–97.

[13] Milles, J.—Zhu, Y.—Gimenez, G.—Guttmann, C.—Magnin, I.: MRI Intensity Nonuniformity Correction Using Simultaneously Spatial and Gray-Level Histogram Information. Computerized Medical Imaging and Graphics, Vol. 31, No. 2, pp. 81–90.

[14] Tincher, M.—Meyer, C. R.—Gupta, R.—Williams, D. M.: Polynomial Modelling and Reduction of RF Body Coil Spatial Inhomogeneity in MRI. IEEE Transactions on Medical Imaging, Vol. 12, 1993, pp. 361–365.

[15] Dawant, B. M.—Zijdenbos, A. P.—Margolin, R. A.: Correction of Intensity Variations in MR Images for Computer-Aided Tissue Classification. IEEE Transactions on Medical Imaging, Vol. 12, 1993, pp. 770–781.

[16] Axel, L.—Costantini, J.—Listerud, J.: Intensity Correction in Surface Coil MR Imaging. American Journal on Roentgenology, Vol. 148, 1987, pp. 418–420.

[17] Brinkmann, B. H.—Manduca, A.—Robb, R. A.: Optimized Homomorphic Unsharp Masking for MR Greyscale Inhomogeneity Correction. IEEE Transactions on Medical Imaging, Vol. 17, 1998, pp. 161–171.

[18] Johnston, B.—Atkins, M. S.—Mackiewich, B.—Anderson, M.: Segmentation of Multiple Sclerosis Lesions in Intensity Corrected Multispectral MRI. IEEE Transaction On Medical Imaging, Vol. 15, 1996, No. 2, pp. 154–169.

[19] Arnold, J. B.—Liow, J. S.—Schaper, K. S.—Stern, J. J.—Sled, J. G.—Shattuck, D. W.—Worth, A. J.—Cohen, M. S.—Leahy, R. M.—Mazziotta, J. C.—Rottenberg, D. A.: Quantitative and Qualitive Evaluation of Six Al-

gorithms for Correcting Intensity Non-Uniformity Effects. Neuroimage, Vol. 13, 2001, No. 5, pp. 931–943.

[20] Mackiewich, B.: Intracranial Boundary Detection and Radio Frequency Correction in Magnetic Resonance Images. Masters thesis, Simon Fraser Univ., Computer Science Dept., Burnaby, British Columbia, Aug. 1995.

[21] Perona, P.—Malik, J.: Scale-Space and Edge Detection Using Anisotropic Diffusion. IEEE Transaction on Pattern Analysis and Machine Intelligence, Vol. 12, 1990, No. 7, pp. 629–639.

[22] Guillemaud, R.: Uniformity Correction with Homomorphic Filtering on Region of Interest. IEEE International Conference on Image Processing, Vol. 2, 1998, pp. 872–875.

[23] Likar, B.—Viergever, M. A.—Pernus, F.: Retrospective Correction of MR Intensity Inhomogeneity by Information Minimization. IEEE Transactions on Medical Imaging, Vol. 20, 2001, pp. 1398–1410.

[24] Kwan, R. K. S.—Evans, A. C.—Pike, G. B.: MRI Simulation-Based Evaluation of Image Processing and Classification Methods. IEEE Transactions on Medical Imaging. Vol. 18, 1999, No. 11, pp. 1085–1097.

[25] Kwan, R. K. S.—Evans, A. C.—Pike, G. B.: An Extensible MRI Simulator for PostProcessing Evaluation. Visualization in Biomedical Computing (VBC'96), Lecture Notes in Computer Science, Vol. 1131, Springer-Verlag 1996, pp. 135–140.

[26] Ashburner, J.—Friston, K.: MRI Sensitivity Correction and Tissue Classification. NeuroImage, Vol. 7, S706, 1998.

[27] `http://www.itk.org/HTML/MRIBiasCorrection.htm`.

[28] Ardizzone, E.—Pirrone, R.—Gambino, O.: Exponential Entropy Driven HUM on Knee MR Images. Proceedings of IEEE XXVII Engineering in Medicine and Biology Conference 2005, Shanghai, China, pp. 1769–1772, ISBN: 0-7803-8740-6.

[29] Ardizzone, E.—Pirrone, R.—Gambino, O.: Fuzzy C-Means Segmentation on Brain MR Slices Corrupted by RF-Inhomogeneity. Lecture Notes in Computer Science; pp. 378–384, ISSN: 0302-9743.

[30] Ardizzone, E.—Pirrone, R.—Gambino, O.: Bias Artifact Suppression on MR Volumes. Computer Methods and Programs in Biomedicine, Vol. 92, pp. 35–53, Elsevier, 2008.

[31] Pena Pina, X.—Bach Cuadra, M.—Kunz, N.—Just, N.—Gruetter, R.—Thiran, J. Ph.: Fast Bias Field Correction for 9.4 Tesla Magnetic Resonance Imaging. 16th European Signal Processing Conference (EUSIPCO-2008), 2008.

[32] Salvado, O.—Wilson, D. L.: Entropy Based Method to Correct Intensity Inhomogeneity in MR Images. Proceedings of the 26th Annual International Conference of the IEEE EMBS, San Francisco, CA, USA September 1–5, 2004.

[33] Salvado, O.—Hillenbrand, C.—Zhang, S.—Wilson, D. L.: Method to Correct Intensity Inhomogeneity in MR Images for Atherosclerosis Characterization. IEEE Transactions on Medical Imaging, Vol. 25, 2006, No. 5, pp. 539–552.

[34] Kubecka, L.—Jan, J.—Kolar, R.: Retrospective Illumination Correction of Retinal Images. International Journal of Biomedical Imaging, Vol. 2010, Article ID 780262, 10 pages.

Edoardo Ardizzone is a Full Professor of computer systems in the Department of Chemical, Management, Computer and Mechanical Engineering of the University of Palermo (Italy), where he teaches image processing at the School of Engineering. His current research interests include image processing and analysis, medical imaging, and image restoration.

Roberto Pirrone received his Master Degree in electronic engineering in 1991. In 1995 he received the Ph. D. in computer and electronic engineering. From 1999 to 2004 he was Assistant Professor of computer engineering in the Education Sciences Faculty at the University of Palermo. From 2005 he is Associate Professor of computer engineering at the same faculty. His research activity is with the Department of Chemical, Management, Computer and Mechanical Engineering of the University of Palermo. He teaches computers Graphics for the course in Computer Engineering at the Engineering Faculty, and foundations of computer science for the course in communication science at the Education Sciences Faculty. His research interests are in design of cognitive architectures applied to intelligent tutoring, semantic approaches for information retrieval and KDD, conversational agents, and medical image analysis and restoration.

Orazio Gambino graduated in computer science engineering at the Department of Computer Science, University of Palermo. He received his Ph. D. in computer science at the same institution with the thesis "Algorithms and Experimentations on Pathological and Normal Encephalic Resonance Images". On 1 December 2008 he became Assistant Professor, SSD ING-INF/05. He teaches foundations of computer science and computer science for institutional and business communication for the course in communication science at the Education Sciences Faculty. His research activity is with the Department of Chemical, Management, Computer and Mechanical Engineering of the University of Palermo. Research interests: artifacts removal on digital and medical images, medical imaging, segmentation, content based image retrieval, graphical user interfaces.

Salvatore Vitabile is Assistant Professor with the Department of Biopathology, Medical and Forensic BiotechNo.logies (DIBIMEF) at the University of Palermo, Italy. He received the Laurea degree in electronic engineering and the doctoral degree in computer science from the University of Palermo in 1994 and 1999, respectively. In 2007, he was a Visiting Professor at the Department of Radiology, Ohio State University, Columbus, OH, USA. His research interests include specialized architecture design and prototyping, neural network applications, biometric authentication systems, real-time driver assistance systems, and medical image processing. He is currently member of the Board of Directors of SIREN (Italian Society of Neural Networks). He is the Editor in Chief of the International Journal of Adaptive and Innovative Systems, Inderscience Publishers, and he has joined the Editorial Board of the International Journal of Information Technology, Communications and Convergence and of the International Journal of Space-Based and Situated Computing.